www.ietdl.org

Published in IET Generation, Transmission & Distribution
Received on 5th October 2012
Revised on 31st January 2013
Accepted on 10th March 2013
doi: 10.1049/iet-gtd.2012.0576

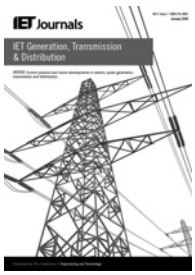

ISSN 1751-8687

Secondary control of microgrids based on distributed cooperative control of multi-agent systems

Ali Bidram[1], Ali Davoudi[2], Frank L. Lewis[1], Zhihua Qu[3]

[1]*The University of Texas at Arlington Research Institute, The University of Texas at Arlington, 7300 Jack Newell Blvd. S., Ft. Worth, TX 76118, USA*
[2]*Electrical Engineering Department, The University of Texas at Arlington, TX, USA*
[3]*Department of Electrical Engineering and Computer Science, University of Central Florida, Orlando, FL 32815 USA*
E-mail: ali.bidram@mavs.uta.edu

Abstract: This study proposes a secondary voltage and frequency control scheme based on the distributed cooperative control of multi-agent systems. The proposed secondary control is implemented through a communication network with one-way communication links. The required communication network is modelled by a directed graph (digraph). The proposed secondary control is fully distributed such that each distributed generator only requires its own information and the information of its neighbours on the communication digraph. Thus, the requirements for a central controller and complex communication network are obviated, and the system reliability is improved. The simulation results verify the effectiveness of the proposed secondary control for a microgrid test system.

1 Introduction

Microgrids as the main building blocks of smart grids are small scale power systems that facilitate the effective integration of distributed generators (DG) [1–6]. In normal operation, the microgrid is connected to the main grid. In the event of disturbances, the microgrid disconnects from the main grid and goes to the islanded operation. Once a microgrid is islanded from the main power grid, the primary control is applied to maintain the voltage and frequency stability [7–9]. However, the primary control can lead to voltage and frequency deviations. To restore the voltage and frequency of the DGs to their nominal value, the secondary control is applied [7, 8, 10–13].

The conventional secondary controls for microgrids assume a centralised structure that requires a complex communication network [7, 8, 10, 11]. The requirements for a central controller and complex communication networks reduce the system reliability. More reliable and sparse communication networks can be accommodated by applying distributed cooperative control to the design of secondary control for microgrids. Compared to a distributed control structure, a centralised control structure is typically more sensitive to failures and error modelling, as it provides a single point-of-failure [14, 15]. Additionally, it should be noted that physical and communication structures of microgrid can be time varying because of the desired plug-and-play capability of microgrids. From this perspective, the distributed control structure provides a robust secondary control framework that appropriately operates in the presence of time varying, restricted, and unreliable communication networks [14]. The cooperative control is recently used to regulate the output power of multiple photovoltaic generators in a power distribution system [16].

Networked multi-agent systems have earned much attention because of their flexibility and computational efficiency over the last two decades. In these systems, the coordination and synchronisation process requires the exchange of information among agents based on some restricted communication protocols [17–20]. Distributed cooperative control of multi-agent systems is mainly categorised into the regulator synchronisation problem and the tracking synchronisation problem. In the regulator synchronisation problem, all agents synchronise to a common value that is not prescribed. In the tracking synchronisation problem, all agents synchronise to a leader that acts as a command generator [21–23].

A microgrid can be considered as a multi-agent system, where each DG is an agent. The secondary control design resembles a tracking synchronisation problem where the DGs terminal voltages and frequencies track voltage and frequency reference values, respectively. The dynamics of DGs in microgrids are nonlinear and non-identical. Thus, input–output feedback linearisation can be used to transform the nonlinear heterogeneous dynamics of DGs to linear dynamics. Once input–output feedback linearisation is applied, the secondary control leads to a first-order tracking synchronisation problem.

This paper makes the following contributions that, to the best of authors' knowledge, have not been exploited yet:

- The secondary control of electric power microgrids is implemented through the concept of distributed cooperative control of multi-agent systems.
- The Lyapunov energy-based technique is adopted to derive fully distributed voltage and frequency control protocols for each DG.
- The proposed secondary control is implemented through a sparse communication network. The communication network is modelled by a directed graph (digraph). Each DG requires its own information and the information of its neighbours on the digraph. Compared to the conventional secondary control with a centralised structure, the proposed secondary control is less sensitive to the failure of communication links.
- The proposed secondary frequency control can restore the microgrid frequency and share the active power among DGs based on their nominal power ratings.

The paper is organised as follows: Section 2 discusses the primary and secondary control levels. In Section 3, the dynamical model of inverter-based DGs is presented. In Section 4, the secondary voltage and frequency controls based on distributed cooperative control of multi-agent systems are presented. The proposed secondary control is verified in Section 5 on a microgrid test system. Section 6 concludes the paper.

2 Microgrid hierarchical control structure

The hierarchical control structure of microgrids is inspired by the three-layer control structure of large-scale power systems. The first layer of a power system control structure provides the balance between the loads and generations at the cost of frequency deviation. This layer is implemented in the governor of each synchronous generator and is referred to as a droop controller. The second layer, referred to as the automatic generation control (AGC), compensates the frequency deviations caused by the droop controllers, and appropriately allocates the output power of generators to control the active power interchanged among different areas [24, 25]. For each area, the area control error (ACE) is defined as

$$\mathrm{ACE} = \Delta P_{\mathrm{a}} + k\Delta f \tag{1}$$

where ΔP_{a} is the deviation of active power balance in each area, k is the frequency bias setting, and Δf is the frequency deviation of the power system. The control command of AGC, ΔP_{c}, that is sent to the governor of each generator is

$$\Delta P_{\mathrm{c}} = -\beta_1\,\mathrm{ACE} - \beta_2 \int \mathrm{ACE}\,\mathrm{d}t \tag{2}$$

where β_1 and β_2 are the proportional-plus-integral (PI) control parameters [25]. The third layer is responsible for the economic dispatch, and optimises the generation of synchronous generators based on their operating costs [24, 25].

Similarly, the hierarchical control structure of microgrids consists of three control levels, namely, primary, secondary and tertiary control levels. The primary control is usually implemented as a local controller at each DG using the droop technique. Droop technique prescribes a desired relation between the frequency and active power, and between the voltage amplitude and reactive power. As opposed to synchronous generators, no governor exists in the inverter-based DGs, and the droop technique is virtually implemented in the internal control loops of DGs. The voltage and frequency droop characteristics are given by

$$\begin{cases} v_{\mathrm{mag}} = V_{\mathrm{n}} - n_Q Q \\ \omega = \omega_{\mathrm{n}} - m_P P \end{cases} \tag{3}$$

where v_{mag} and ω are the voltage amplitude and frequency of the DG generated by the primary control. P and Q are the measured active and reactive power at the DGs terminal. m_P and n_Q are the droop coefficients that are usually selected based on the active and reactive power rating of the DG. V_{n} and ω_{n} are the primary control references [7, 8].

The secondary control sets the references V_{n} and ω_{n} in (3) to regulate the voltage amplitude and frequency to their prescribed nominal values. Conventionally, the secondary control is implemented by using a centralised controller for the whole microgrid having the PI structure

$$\begin{cases} \delta V_{\mathrm{n}} = K_{PE}\left(v_{\mathrm{ref}} - v\right) + K_{IE}\int (v_{\mathrm{ref}} - v)\,\mathrm{d}t \\ \delta\omega_{\mathrm{n}} = K_{P\omega}\left(\omega_{\mathrm{ref}} - \omega\right) + K_{I\omega}\int (\omega_{\mathrm{ref}} - \omega)\,\mathrm{d}t \end{cases} \tag{4}$$

where $\delta\omega_{\mathrm{n}}$ and δV_{n} are the commands sent to the primary control of the DG, v_{ref} and ω_{ref} are the nominal values for the voltage and frequency, and v and ω are the voltage amplitudes and frequency in the microgrid, monitored by the centralised controller. The controller parameters are $K_{P\omega}$, $K_{I\omega}$, K_{PE}, and K_{IE} [7, 8]. The block diagram of the conventional secondary control is shown in Fig. 1. It should be noted that in large scale power systems, AGC provides an additional power demand signal to the set point of the governor. However, the command signal of the secondary control of microgirds alters the primary control references V_{n} and ω_{n} to compensate the frequency and voltage deviations.

In a centralised control structure, seen in Fig. 2*a*, the central controller communicates with all DGs in the microgrid through a star communication network. A centralised control structure decreases the system reliability. In Section 4, the distributed cooperative control of multi-agent systems will be adopted to develop a more efficient secondary control with distributed structure, as shown in Fig. 2*b*.

Tertiary control considers the economic concerns in the optimal operation of the microgrid, and manages the power flow between microgrid and main grid. Interested readers can find further information about the tertiary control level in [7, 8].

3 Dynamical model of inverter-based DG

Fig. 3*a* shows the block diagram of an inverter-based DG. It contains the primary power source (e.g. photovoltaic panels), the voltage source converter (VSC), and the power, voltage, and current control loops. The control loops set and control the output voltage and frequency of the VSC. Outer voltage controller and inner current controller block diagrams are elaborated in [26]. The power controller contains the droop technique in (3) and provides the voltage references v_{od}^* and v_{oq}^* for the voltage controller, and the operating frequency ω for the VSC, seen in Fig. 3*b*. Note that the nonlinear dynamics of each DG in a microgrid are formulated on its own direct-quadratic (d–q) reference frame. The reference frame of one DG is considered as the common reference frame and the dynamics of other DGs are transformed to the common reference frame. The

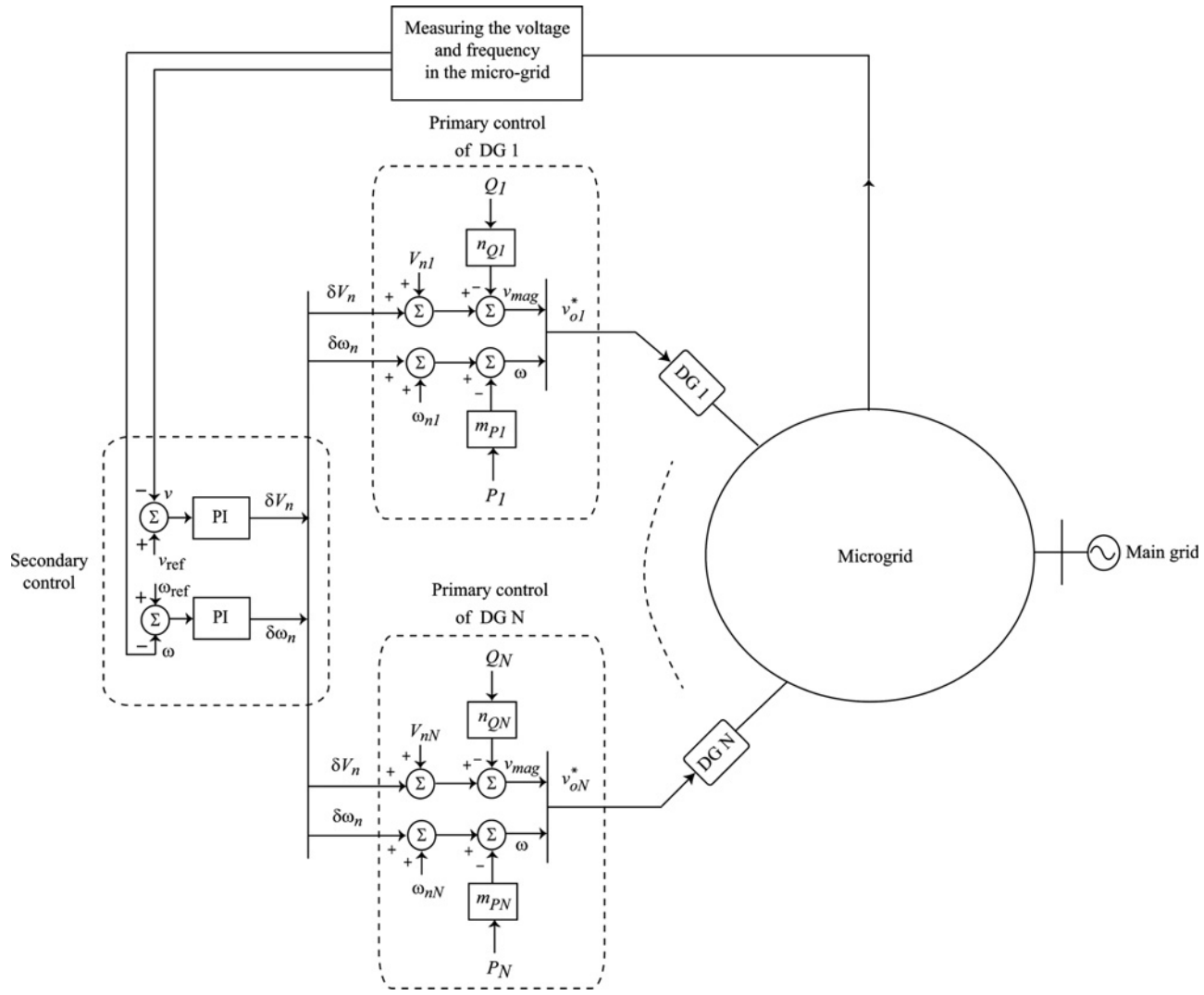

Fig. 1 *Conventional secondary control*

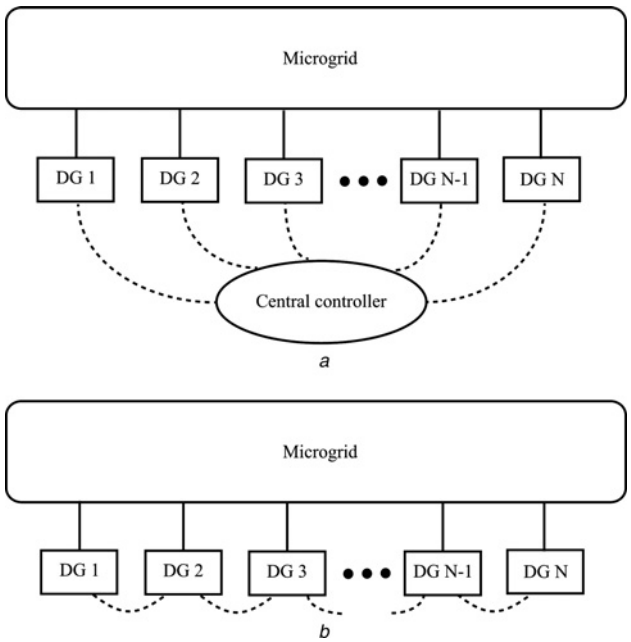

Fig. 2 *Secondary control structures*

a Centralised
b Distributed

angular frequency of this common reference frame is denoted by ω_{com}.

The primary voltage control strategy is to align the voltage magnitude of each DG on the d-axis of its reference frame. Therefore for the ith DG

$$\begin{cases} v_{odi}^{*} = V_{\text{ni}} - n_{Qi}Q_i \\ v_{oqi}^{*} = 0 \end{cases} \tag{5}$$

The secondary voltage control selects V_{ni} in Fig. 3*b* such that the terminal voltage amplitude of each DG synchronises to its nominal value, that is $v_{\text{o,magi}} \rightarrow v_{\text{ref}}$. Since the amplitude of the DG output voltage is

$$v_{\text{o,magi}} = \sqrt{v_{odi}^2 + v_{oqi}^2} \tag{6}$$

according to (5), the synchronisation for the voltage amplitude of DGs is achieved by choosing the control input V_{ni} such that $v_{odi} \rightarrow v_{\text{ref}}$. The secondary frequency control is to choose ω_{ni} in Fig. 3*b* such that the angular frequency of each DG synchronises to its nominal value, that is $\omega_i \rightarrow \omega_{\text{ref}}$.

doi: 10.1049/iet-gtd.2012.0576

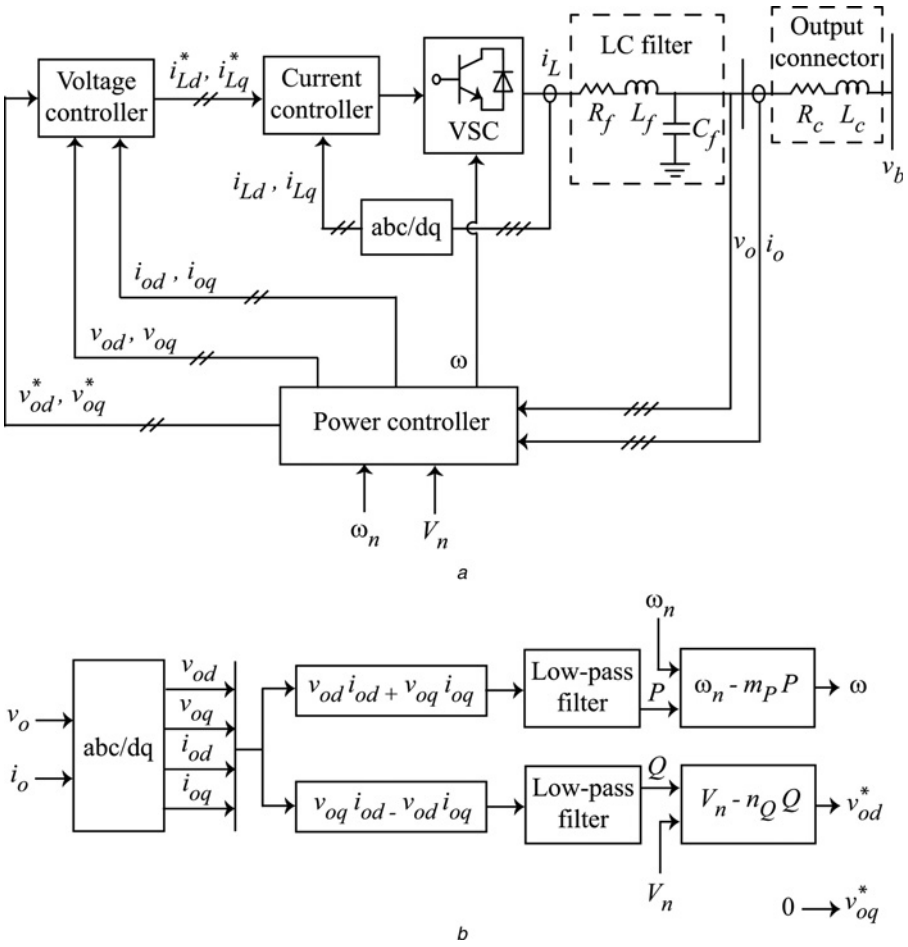

Fig. 3 *An inverter-based DG*

a Block diagram of an inverter-based DG
b Block diagram of the power controller

The nonlinear dynamics of the *i*th DG, shown in Fig. 3*a*, can be written as

$$\begin{cases} \dot{\boldsymbol{x}}_i = \boldsymbol{f}_i(\boldsymbol{x}_i) + \boldsymbol{k}_i(\boldsymbol{x}_i)\boldsymbol{D}_i + \boldsymbol{g}_i(\boldsymbol{x}_i)u_i \\ y_i = h_i(\boldsymbol{x}_i) + d_i u_i \end{cases} \tag{7}$$

where the state vector is (see (8))

δ_i is the angle of the DG reference frame with respect to the common reference frame. P_i and Q_i are the filtered output active and reactive power (see Fig. 3*b*). ϕ_{di} and ϕ_{qi} are the direct and quadratic components of the auxiliary variable for the voltage controller. γ_{di} and γ_{qi} are the direct and quadratic components of the auxiliary variable for the current controller. i_{Ldi}, i_{Lqi}, v_{odi}, v_{oqi}, i_{odi}, and i_{oqi} are the direct and quadratic components of i_{Li}, v_{oi}, and i_{oi} in Fig. 3*a*, respectively.

The term $\boldsymbol{D}_i = \begin{bmatrix} \omega_{com} & v_{bdi} & v_{bqi} \end{bmatrix}^{\mathrm{T}}$ is considered as a known disturbance. For the secondary voltage control, the outputs and inputs are $y_i = v_{odi}$ and $u_i = V_{ni}$, respectively. For the secondary frequency control, the outputs and inputs are $y_i = \omega_i$ and $u_i = \omega_{ni}$, respectively. The detailed expressions for $\boldsymbol{f}_i(\boldsymbol{x}_i)$, $\boldsymbol{g}_i(\boldsymbol{x}_i)$, $h_i(\boldsymbol{x}_i)$, d_i, and $\boldsymbol{k}_i(\boldsymbol{x}_i)$ are adopted from the nonlinear model presented in [26].

4 Secondary control based on distributed cooperative control

The secondary control of microgrids is a tracking synchronisation problem, where all DGs try to synchronise their terminal voltage amplitude and frequency to pre-specified reference values. In the tracking synchronisation problem, all agents seek to synchronise to a leader that acts as a command generator [21, 27]. For this purpose, each DG needs to communicate with its neighbours and receive the information of neighbouring DGs (see Fig. 2*b*). The required communication network can be modelled by a communication digraph.

4.1 Preliminaries on graph theory

The communication network of a microgrid can be modelled by a digraph. In a microgrid, DGs are considered as the nodes of the communication digraph. The edges of the corresponding digraph of the communication network denote the communication links. A digraph is usually expressed as $\mathcal{G} = (\mathcal{V}, \mathcal{E}, \mathcal{A})$ with a non-empty finite set of N nodes $\mathcal{V} = \{v_1, v_2, \ldots, v_N\}$, a set of edges or arcs $\mathcal{E} \subset \mathcal{V} \times \mathcal{V}$, and the associated adjacency matrix $\mathcal{A} = [a_{ij}] \in \mathbb{R}^{N \times N}$. In this paper, the digraph is assumed to

$$\boldsymbol{x}_i = \begin{bmatrix} \delta_i & P_i & Q_i & \phi_{di} & \phi_{qi} & \gamma_{di} & \gamma_{qi} & i_{Ldi} & i_{Lqi} & v_{odi} & v_{oqi} & i_{odi} & i_{oqi} \end{bmatrix}^{\mathrm{T}} \tag{8}$$

be time-invariant, that is $\mathcal{A}$ is constant. An edge from node j to node i is denoted by (v_j, v_i), which means that node i receives the information from node j. a_{ij} is the weight of edge (v_j, v_i), and $a_{ij} > 0$ if $(v_j, v_i) \in \mathcal{E}$, otherwise $a_{ij} = 0$. Node j is called a neighbour of node i if $(v_j, v_i) \in \mathcal{E}$. The set of neighbours of node i is denoted as $N_i = \{j | (v_j, v_i) \in \mathcal{E}\}$. For a digraph, if node j is a neighbour of node i, then node i can obtain information from node j, but not necessarily vice versa. The in-degree matrix is defined as $\boldsymbol{D} = \text{diag}\{d_i\} \in \mathbb{R}^{N\times N}$ with $d_i = \sum_{j\in N_i} a_{ij}$. The Laplacian matrix is defined as $L = \boldsymbol{D} - \mathcal{A}$. L has all row sums equal to zero, that is $L\mathbf{1}_N = 0$, with $\mathbf{1}_N$ being the vector of ones with the length of N.

A directed path from node i to node j is a sequence of edges, expressed as $\{(v_i, v_k), (v_k, v_l), \ldots, (v_m, v_j)\}$. A digraph is said to have a spanning tree, if there is a node i_r (called the root), such that there is a directed path from the root to every other node in the graph [28].

4.2 Distributed cooperative voltage control

In this section, a distributed cooperative control is designed to synchronise the voltage magnitudes of DGs $v_{o,magi}$ to the reference voltage v_{ref}. According to Section 3, the synchronisation of the voltage magnitudes of DGs $v_{o,magi}$ is equivalent to synchronising the direct term of output voltages v_{odi}. The secondary voltage control is to choose appropriate control inputs V_{ni} for the droop characteristic in (3) based on the following procedure.

The nonlinear dynamics of the ith DG, seen in (7), are considered. It should be noted that the dynamics of the voltage and current controller are much faster than the dynamics of the power controller [26]. Therefore by neglecting the fast dynamics of the voltage and current controller, (5) can be written as

$$\begin{cases} v_{odi} = V_{ni} - n_{Qi}Q_i \\ v_{oqi} = 0 \end{cases} \tag{9}$$

Differentiating the upper equation in (9) yields

$$\dot{v}_{odi} = \dot{V}_{ni} - n_{Qi}\dot{Q}_i \equiv u_{vi} \tag{10}$$

where u_{vi} is an auxiliary control. This process is called as input–output feedback linearisation [29]. Equation (10) is a dynamic system for computing the control input V_{ni} in (3) from u_{vi}. According to (10), the secondary voltage control of a microgrid including N DGs is transformed to the tracking synchronisation problem for a first-order and linear multi-agent system

$$\begin{cases} \dot{v}_{od1} = u_{v1} \\ \dot{v}_{od2} = u_{v2} \\ \vdots \\ \dot{v}_{odN} = u_{vN} \end{cases} \tag{11}$$

To achieve the synchronisation for v_{odi}, it is assumed that DGs can communicate with each other through a prescribed communication digraph $\mathcal{G}$. The auxiliary controls u_{vi} are chosen based on the own information of each DG and the information of its neighbours in the graph as

$$u_{vi} = -c_v e_{vi} \tag{12}$$

where the control gain is $c_v \in \mathbb{R}$ and e_{vi} is the local neighbourhood tracking error

$$e_{vi} = \sum_{j\in N_i} a_{ij}\left(v_{odi} - v_{odj}\right) + g_i\left(v_{odi} - v_{ref}\right) \tag{13}$$

The pinning gain $g_i \geq 0$ is the weight of the edge by which ith DG is connected to the reference. The elements of the adjacency matrix $\mathcal{A}$ are denoted by a_{ij}. Any change in the communication network will be reflected in the adjacency matrix $\mathcal{A}$. Therefore the coefficients a_{ij} in (13) must be altered accordingly. For example suppose that a new DG, namely 'DG $N+1$', is installed in the microgrid, and this DG is a neighbour of 'DG i' on the communication digraph, that is 'DG $N+1$' sends its information to 'DG i' through an edge with the weight factor a_{iN+1}. In this situation, the additional term $a_{iN+1}(v_{odi} - v_{odN+1})$ would be added to the local neighbourhood tracking error of 'DG i', whereas the local neighbourhood tracking error of other DGs stay intact. The pinning gain is non-zero only for a few DGs (at least one DG) that are given the reference voltage v_{ref}. The communication digraph shown in Fig. 4*a* can be considered for a typical microgrid including four DGs. Fig. 4*b* illustrates the communication network required to implement the secondary voltage control in this microgrid.

To prove that the proposed controller in (12) can provide the synchronisation for v_{odi}, the following lemmas and theorem are considered. From (13), the global neighbourhood error vector for graph $\mathcal{G}$ is written as

$$\boldsymbol{e} = (L + G)\left(\boldsymbol{v}_{od} - \boldsymbol{v}_{ref}\right) \equiv (L + G)\boldsymbol{\delta} \tag{14}$$

where the global variables are defined as $\boldsymbol{v}_{od} = \begin{bmatrix} v_{od1} & v_{od2} & \cdots & v_{odN} \end{bmatrix}^{\mathrm{T}}$, $\boldsymbol{e} = \begin{bmatrix} e_{v1} & e_{v2} & \cdots & e_{vN} \end{bmatrix}^{\mathrm{T}}$, and, $\boldsymbol{v}_{ref} = \mathbf{1}_N \otimes v_{ref}$ with $\mathbf{1}_N$ the vector of ones with the length of N. The Kronecker product is $\otimes$. $G \in \mathbb{R}^{N\times N}$ is a diagonal matrix with diagonal entries equal to the pinning gains g_i. The global disagreement vector is $\boldsymbol{\delta}$.

Lemma 1 [30]: Let the digraph $\mathcal{G}$ have a spanning tree and $g_i \neq 0$ for at least one root node. Then

$$||\boldsymbol{\delta}|| \leq ||\boldsymbol{e}||/\sigma_{\min}(L + G) \tag{15}$$

where $\sigma_{\min}(L + G)$ is the minimum singular value of $L + G$, and $\boldsymbol{e} = 0$ if and only if all nodes synchronise.

Lemma 2 [28]: Let the digraph $\mathcal{G}$ have a spanning tree and $g_i \neq 0$ for at least one root node. Let $P = \text{diag}\{1/w_i\}$, where w_i are the elements of a vector $\boldsymbol{w}$ that satisfies $\boldsymbol{A}\boldsymbol{w} = \mathbf{1}_N$, where $\boldsymbol{A} \equiv L + G$. Then, $Q \equiv P\boldsymbol{A} + \boldsymbol{A}^{\mathrm{T}}P$ is positive definite.

Theorem 1: Let the digraph $\mathcal{G}$ have a spanning tree and $g_i \neq 0$ for at least one DG. Let the auxiliary control u_{vi} be chosen as in (12). Then, the global neighbourhood error $\boldsymbol{e}$ in (14) is asymptotically stable. Moreover, the DG output voltage direct terms v_{odi} synchronise to v_{ref}.

Proof: From (12), the global input vector $\boldsymbol{u}_v$ is

$$\boldsymbol{u}_v = \begin{bmatrix} u_{v1} & u_{v2} & \cdots & u_{vN} \end{bmatrix}^{\mathrm{T}} = -c_v\boldsymbol{e} \tag{16}$$

doi: 10.1049/iet-gtd.2012.0576

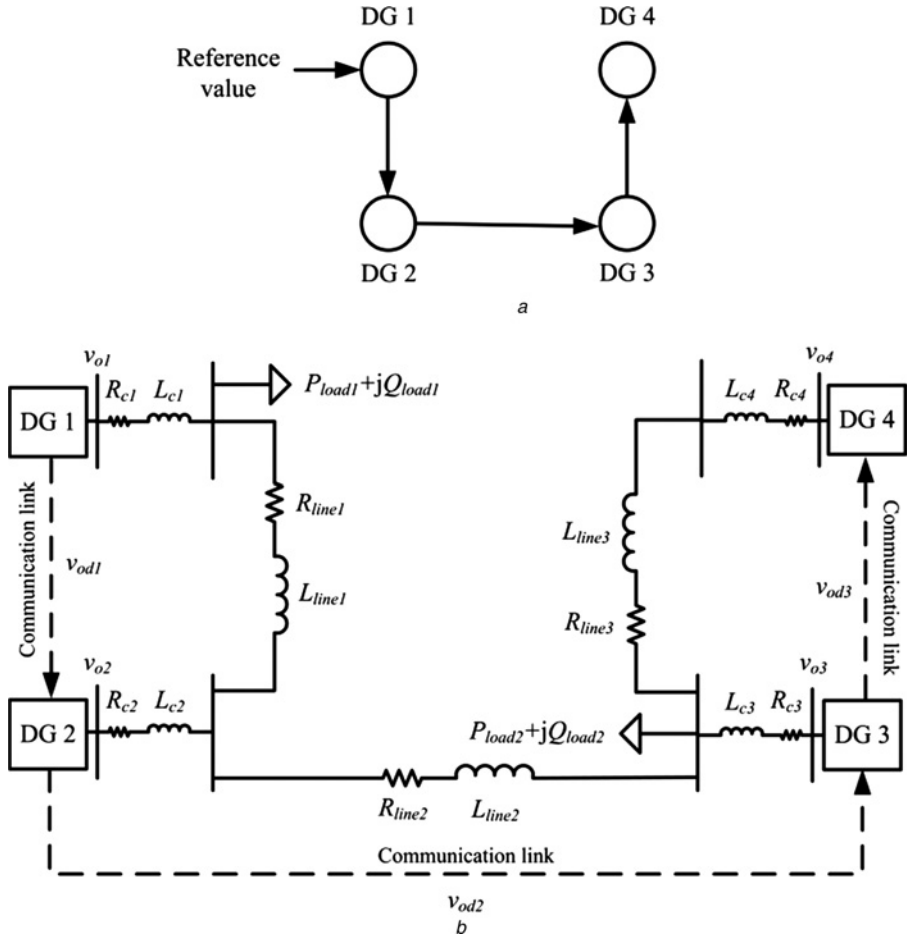

Fig. 4 *Communication structure for the distributed cooperative secondary voltage control of the example microgrid*
a Communication network digraph;
b Implemented communication network on the microgrid

Consider the Lyapunov function candidate

$$V = \frac{1}{2}\boldsymbol{e}^{\mathrm{T}}P\boldsymbol{e}, \quad P = P^{\mathrm{T}}, \quad P > 0 \tag{17}$$

then, using (14) and $\dot{\boldsymbol{v}}_{od} = \boldsymbol{u}_v$ yields

$$\dot{V} = \boldsymbol{e}^{\mathrm{T}}P\dot{\boldsymbol{e}} = \boldsymbol{e}^{\mathrm{T}}P(L+G)(\dot{\boldsymbol{v}}_{od}) = \boldsymbol{e}^{\mathrm{T}}P(L+G)(\boldsymbol{u}_v) \tag{18}$$

Defining $\boldsymbol{A} \equiv L + G$, and placing (16) into (18) yields

$$\dot{V} = -c_v\boldsymbol{e}^{\mathrm{T}}P\boldsymbol{A}\boldsymbol{e} = \frac{-c_v}{2}\boldsymbol{e}^{\mathrm{T}}\left(P\boldsymbol{A} + \boldsymbol{A}^{\mathrm{T}}P\right)\boldsymbol{e} \tag{19}$$

From Lemma 2, the matrix $Q \equiv P\boldsymbol{A} + \boldsymbol{A}^{\mathrm{T}}P$ is positive definite. Therefore the term $(-c_v/2)\boldsymbol{e}^{\mathrm{T}}Q\boldsymbol{e}$ is negative definite and the global neighbourhood error $\boldsymbol{e}$ is asymptotically stable. From Lemma 1, the global disagreement vector $\boldsymbol{\delta}$ is asymptotically stable and the DG output voltage direct terms v_{odi} synchronise to v_{ref}. This completes the proof.

Remark 1: Equation (19) yields

$$\dot{V} \le \frac{-c_v}{2}\sigma_{\min}(Q)\|e\|^2 \le \frac{-c_v}{2}\frac{\sigma_{\min}(Q)}{\sigma_{\max}(P)}V \equiv -2\alpha V \tag{20}$$

where $\sigma_{\max}(P)$ is the maximum singular value of P. From (20), one can write

$$V \le \mathrm{e}^{-2\alpha t}V(t_0) \tag{21}$$

where t_0 is the time instant that the secondary control is applied. From (17) and (21)

$$\frac{1}{2}\sigma_{\min}(P)\left\|\boldsymbol{e}(t)\right\|^2 \le \frac{1}{2}\sigma_{\max}(P)\mathrm{e}^{-2\alpha t}\left\|\boldsymbol{e}(t_0)\right\|^2 \tag{22}$$

or equivalently

$$\left\|\boldsymbol{e}(t)\right\| \le \sqrt{\frac{\sigma_{\max}(P)}{\sigma_{\min}(P)}}\mathrm{e}^{-\alpha t}\left\|\boldsymbol{e}(t_0)\right\| \tag{23}$$

Equation (23) shows that the global neighbourhood error $\boldsymbol{e}(t)$ goes to zero with the time constant $1/\alpha$. Since $\alpha = (c_v/4)(\sigma_{\min}(Q)/\sigma_{\max}(P))$, the synchronisation speed of the secondary voltage control can be adjusted by c_v.

The block diagram of the secondary voltage control based on the distributed cooperative control is shown in Fig. 5. The control input $V_{\mathrm{n}i}$ is written as

$$V_{\mathrm{n}i} = \int\left(u_{vi} + n_{Qi}\dot{Q}_i\right)\mathrm{d}t \tag{24}$$

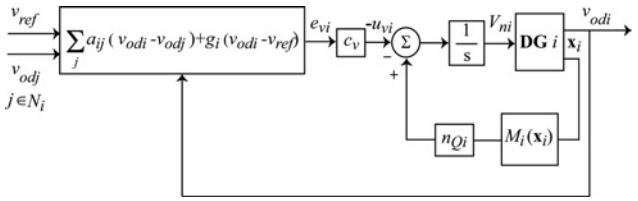

Fig. 5 *Block diagram of the distributed cooperative secondary voltage control*

where adopted from [26], $\dot{Q}_i$ is

$$\dot{Q}_i = -\omega_c Q_i + \omega_c\left(v_{oqi} i_{odi} - v_{odi} i_{oqi}\right) \equiv M_i(\boldsymbol{x}_i) \tag{25}$$

where ω_c is the cut-off frequency of the low-pass filters in Fig. 3*b*.

4.3 Distributed cooperative frequency control

In this section, a distributed cooperative control is designed to synchronise the frequency of DGs ω_i to the reference frequency ω_{ref}. The secondary frequency control is to choose appropriate control inputs ω_{ni} based on the following procedure.

The nonlinear dynamics of the ith DG, seen in (7), are considered. Differentiating the frequency droop characteristic in (3), yields

$$\dot{\omega}_i = \dot{\omega}_{ni} - m_{Pi}\dot{P}_i = u_{\omega i} \tag{26}$$

where $u_{\omega i}$ is an auxiliary control to be designed. Equation (26) is a dynamic system for computing the control input ω_{ni} in (3) from $u_{\omega i}$ (see Fig. 6). According to (26), the secondary frequency control of a microgrid including N DGs is transformed to a tracking synchronisation problem for a first-order and linear multi-agent system

$$\begin{cases} \dot{\omega}_1 = u_{\omega 1} \\ \dot{\omega}_2 = u_{\omega 2} \\ \vdots \\ \dot{\omega}_N = u_{\omega N} \end{cases} \tag{27}$$

To achieve the synchronisation, it is assumed that DGs can communicate with each other through the prescribed communication digraph $\mathcal{G}$. The auxiliary controls $u_{\omega i}$ are chosen based on the each DGs own information, and the information of its neighbours in the communication digraph as

$$u_{\omega i} = -c_\omega e_{\omega i} \tag{28}$$

where $c_\omega \in \mathbb{R}$ and $e_{\omega i}$ is the local neighbourhood tracking error

$$e_{\omega i} = \sum_{j \in N_i} a_{ij}\left(\omega_i - \omega_j\right) + g_i\left(\omega_i - \omega_{\text{ref}}\right) \tag{29}$$

Theorem 1 can be slightly modified to prove that the proposed controller in (28) provides the synchronisation.

According to (26) and (28), ω_{ni} is written as

$$\omega_{ni} = \int \left(u_{\omega i} + m_{Pi}\dot{P}_i\right) \mathrm{d}t \tag{30}$$

This structure is shown in Fig. 6.

It should be noted that once the secondary frequency control is applied, the DG output powers are expected to be allocated according to the same pattern used for primary control [31]. After applying the primary control, the DG output powers satisfy the following equality

$$m_{P1}P_1 = \cdots = m_{PN}P_N \tag{31}$$

Since the active power droop coefficients m_{Pi} are chosen based on the active power rating of DGs, $P_{\max,i}$, (31) is equivalent to

$$\frac{P_1}{P_{\max 1}} = \cdots = \frac{P_N}{P_{\max N}} \tag{32}$$

Therefore the secondary frequency control must also satisfy (31) and (32) [31]. This requirement can be met by considering an additional distributed cooperative control for $m_{Pi}\dot{P}_i$ in (30). This distributed cooperative problem is a regulator synchronisation problem for the linear and first-order multi-agent system

$$\begin{cases} m_{P1}\dot{P}_1 = u_{p1} \\ m_{P2}\dot{P}_2 = u_{p2} \\ \vdots \\ m_{PN}\dot{P}_N = u_{pN} \end{cases} \tag{33}$$

To achieve synchronisation, it is assumed that DGs can communicate with each other through the prescribed communication digraph $\mathcal{G}$. The auxiliary controls u_{pi} are chosen based on the own information of each DG and the information of its neighbours in the communication digraph as

$$u_{pi} = -c_p e_{pi} \tag{34}$$

where $c_p \in \mathbb{R}$ and e_{pi} is local neighbourhood tracking error

$$e_{pi} = \sum_{j \in N_i} a_{ij}\left(m_{Pi}P_i - m_{Pj}P_j\right) \tag{35}$$

Compared to e_{vi} and $e_{\omega i}$ in (13) and (29), there is no second term with pinning gain g_i to a reference value. Therefore Theorem 1 can be modified to prove that the proposed controller in (34) satisfies (31) and (32) without a particular final synchronisation value.

The block diagram of the secondary frequency control based on the distributed cooperative control is shown in

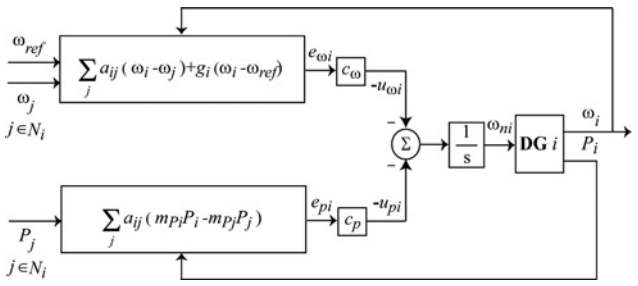

Fig. 6 *Block diagram of the distributed cooperative secondary frequency control*

doi: 10.1049/iet-gtd.2012.0576

Fig. 6. As seen in this figure, the control input ω_{ni} is written as

$$\omega_{ni} = \int \left(u_{\omega i} + u_{pi}\right) \mathrm{d}t \tag{36}$$

The control gains c_ω and c_p can tune the convergence speed of DG frequencies and filtered output power.

4.4 Sparse efficient communication topology for secondary control

The distributed cooperative secondary control must be supported by a local communication network that provides its required information flows. This communication graph should be designed to reduce transmission delays and the required information flows between components. For the microgrids with a small geographical span, the communication network can be implemented by CAN Bus and PROFIBUS communication protocols [11, 32]. It should be noted that communication links contain an intrinsic delay; however, since the time scale of the secondary control is large enough, the communication link delays do not affect the system performance [11].

According to the results of Theorem 1, the communication requirements for implementing the proposed secondary control are rather mild. Specifically, the communication topology should be a graph containing a spanning tree in which the secondary control of each DG only requires information about that DG and its direct neighbours in the communication graph. Given the physical structure of the microgrid, it is not difficult to select a graph with a spanning tree that connects all DGs in an optimal fashion. Such optimal connecting graphs can be designed using operations research or assignment problem solutions [33, 34]. The optimisation criteria can include minimal lengths of the communication links, maximal use of existing communication links, minimal number of links, and so on.

Since a centralised structure provides a single point-of-failure, the proposed framework is more reliable than existing centralised secondary controls. Additionally, in a centralised control structure, the secondary control is lost for a DG if the communication link between the central controller and that DG fails. However, in a distributed control structure, the secondary control is not lost for DGs with communication link failures as long as the communication digraph still contains a spanning tree.

5 Case studies

The microgrid shown in Fig. 4*b* is used to verify the effectiveness of the proposed secondary control. This microgrid consists of four DGs. The lines between buses are modelled as series RL branches. The specifications of

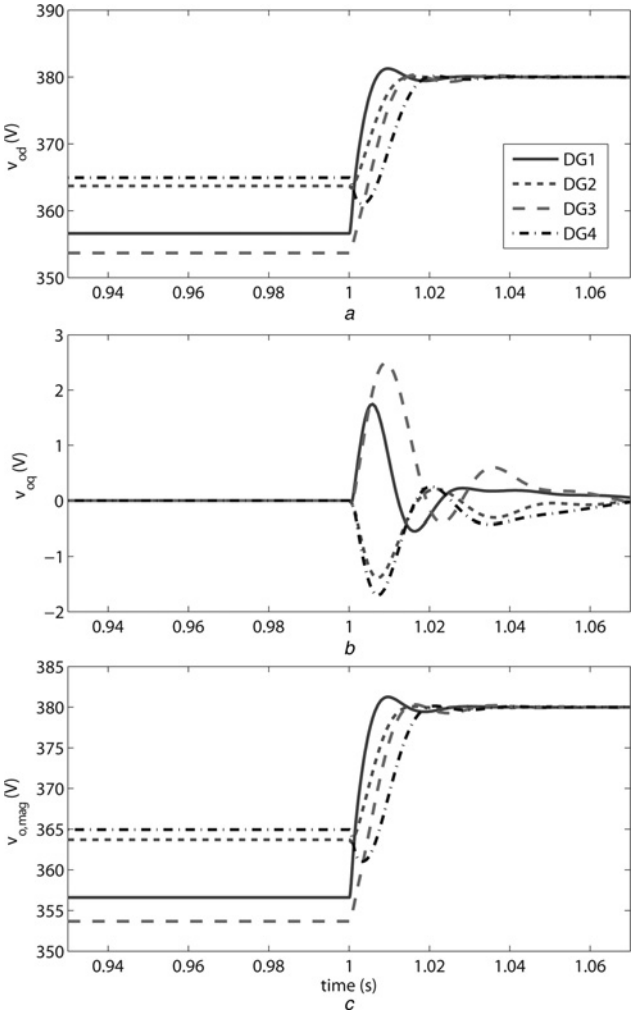

Fig. 7 *Secondary voltage control with $v_{ref} = 380$ v*
a DG output voltage direct terms
b DG output voltage quadratic terms
c DG output voltage magnitudes

Table 1 Specifications of the microgrid test system

DGs	DG 1 & 2 (33 kVA rating)				DG 3 & 4 (25 kVA rating)				
	m_P 9.4×10^{-5}		n_Q 1.3×10^{-3}		m_P 12.50×10^{-5}		n_Q 1.5×10^{-3}		
	R_c 0.03 Ω		L_c 0.35 ml-l		R_c 0.03 Ω		L_c 0.35 mH		
	K_{PV} 0.1	K_{IV} 420	K_{PC} 15	K_{IC} 20000	K_{PV} 0.05	K_{IV} 390	K_{PC} 10.5	K_{IC} 16000	
Lines	Line 1		Line 2		Line 3				
	R_{line1} 0.23 Ω	L_{line1} 0.318 mH	R_{line2} 0.35 Ω	L_{line2} 1.847 mH	R_{line3} 0.23 Ω	L_{line3} 0.318 mH			
Loads	Load 1				Load 2				
	P_{load1} (per phase) 12 kW		Q_{load1} (per phase) 12 kVAr		P_{load2} (per phase) 15.3 kW		Q_{load2} (per phase) 7.6 kVAr		

the DGs, lines, and loads are summarised in Table 1. In this table, K_{PV}, K_{IV}, K_{PC}, and K_{IC} are the parameters of the voltage and current controllers in Fig. 3*a*. The voltage and current controller parameters are adopted from [26]. The simulation results are extracted by modelling the dynamical equations of microgrid in Matlab.

It is assumed that the DGs communicate with each other through the communication digraph depicted in Fig. 4*a*. This communication topology is chosen based on the geographical location of DGs. The associated adjacency matrix of the digraph in Fig. 4*a* is

$$\mathcal{A} = \begin{bmatrix} 0 & 0 & 0 & 0 \\ 1 & 0 & 0 & 0 \\ 0 & 1 & 0 & 0 \\ 0 & 0 & 1 & 0 \end{bmatrix} \tag{37}$$

DG 1 is the only DG that is connected to the leader node with the pinning gain of $g_1 = 1$. In the following, the proposed secondary control method returns the DG voltage amplitudes and frequency of the islanded microgrid to their nominal values. Then, the effect of the control gains c_v, c_ω, and c_p on the response speed of the controllers are investigated.

5.1 Voltage and frequency restoration in microgrid

In this case, the reference value for the terminal voltage of DGs and microgrid angular frequency v_{ref} and ω_{ref} are set as 380 and 314.16 rad/s, respectively (The nominal frequency of the microgrid is 50 z.). The control gains c_v, c_ω, and c_p in (12), (28), and (34) are all set to 400.

It is assumed that the microgrid is islanded form the main grid at $t = 0$. As seen in Fig. 7, after islanding, the direct term of the DG output voltages v_{odi} and the DG terminal voltage amplitudes $v_{\text{o,magi}}$ go to different values less than v_{ref}. The secondary control is applied at $t = 1$ s. Owing to the primary control structure, the quadratic terms of the DG output voltages v_{oqi} converge to 0. Once the proposed secondary control is applied, the direct and quadratic terms of the DG output voltages, v_{odi} and v_{oqi}, synchronise to 1 and 0 pu, respectively. The secondary control returns all of the DG terminal voltage amplitudes to v_{ref} after 0.06. Fig. 8 shows the DG frequencies and output powers before and after applying the secondary frequency control. As seen in Fig. 8*a*, once the primary control is applied, DG operating frequencies all go to a common value, that is the operating frequency of microgrid. However, the secondary frequency control returns the operating frequency of microgrid to its nominal value after 0.3. Fig. 8*b* shows that the DG output powers all satisfy (31) and (32), and are set based on the nominal power of DGs.

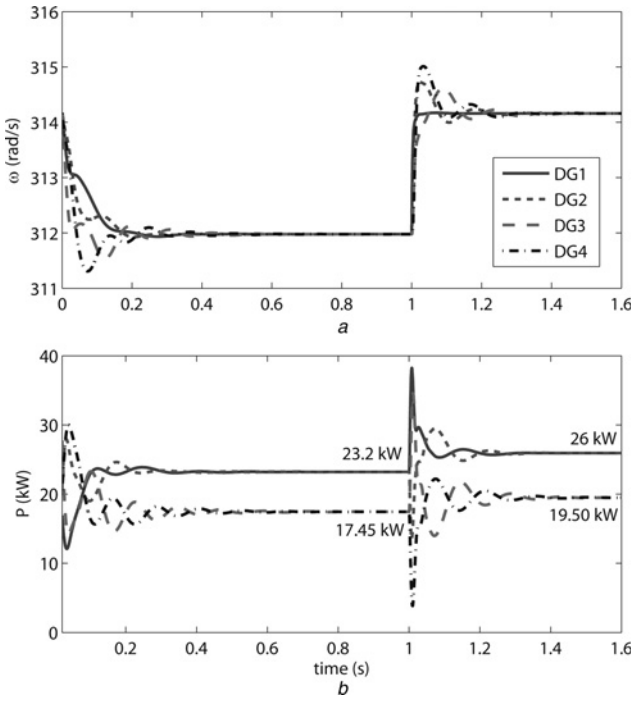

Fig. 8 *Secondary frequency control with $\omega_{ref} = 314.16$ rad/s*
a DG angular frequencies
b DG output powers

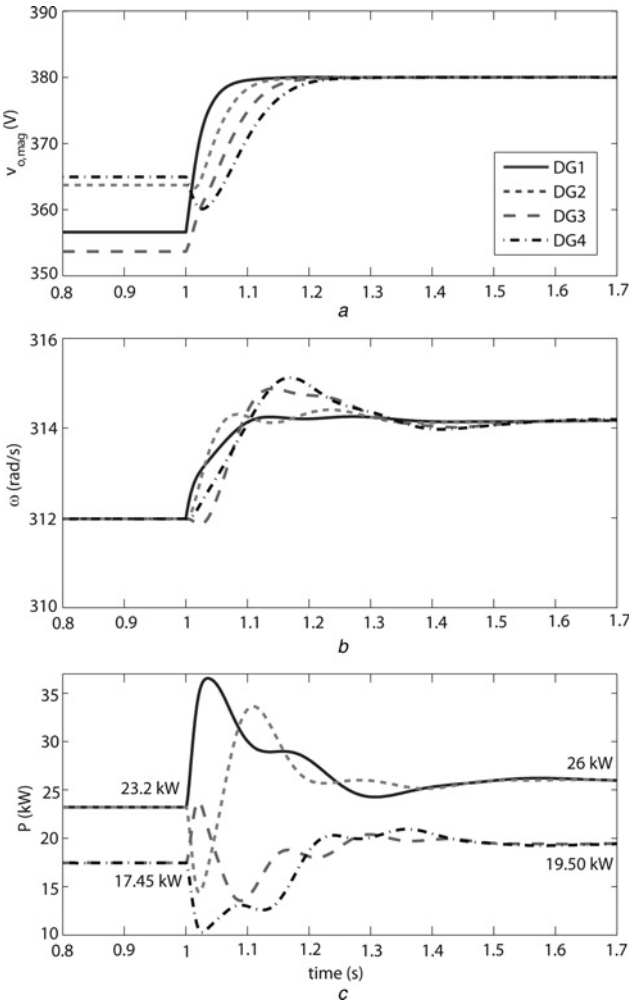

Fig. 9 *Secondary control with $c_v = c_\omega = c_p = 40$*
a DG output voltage magnitudes
b DG angular frequencies
c DG output powers

5.2 Effect of control gains on the transient response

As discussed in Remark 1, the controller gains c_v, c_ω, and c_p in (12), (28), and (34) can adjust the response speed of the secondary control. Fig. 9 shows the secondary control simulation results when v_{ref} and ω_{ref} are set to 380 and 314.16 rad/s, and the control gains are all set to 40. The control gains in this case study are smaller than the

doi: 10.1049/iet-gtd.2012.0576

controller gains in Section 5.1. Compared to Fig. 7*c*, the DG output voltage amplitudes in Fig. 9*a* converge to v_{ref} more slowly. The angular frequency and output power of DGs in Figs. 9*b* and *c* also converge slower compared to those in Figs. 8*a* and *b*.

6 Conclusion

The secondary voltage and frequency control of microgrids are designed based on the distributed cooperative control of multi-agent systems. The microgrid is considered as a multi-agent system with DGs as its agents. DGs can communicate with each other through a communication network modelled by a digraph. Input–output feedback linearisation is used to transform the nonlinear dynamics of DGs to linear dynamics. Feedback linearisation converts the secondary voltage and frequency controls to first-order tracking synchronisation problems. The control inputs are designed such that each DG only requires its own information and the information of its neighbours on the communication digraph. The proposed secondary control structure requires a sparse communication structure and is more reliable than centralised secondary controls.

7 Acknowledgments

This work is supported in part by the NSF under grant numbers ECCS-1137354 and ECCS-1128050, by the AFOSR under grant number FA9550-09-1-0278, by the ARO under grant number W91NF-05-1-0314, and by the China NNSF under grant number 61120106011.

8 References

1 Fahimi, B., Kwasinski, A., Davoudi, A., Balog, R.S., Kiani, M.: 'Charge it', *Power Energy Mag.*, 2011, **9**, (4), pp. 54–64
2 Tanaka, K., Oshiro, M., Toma, S., *et al.*: 'Decentralised control of voltage in distribution systems by distributed generators', *IET Gener., Transm. Distrib.*, 2010, **4**, (11), pp. 1251–1260
3 Rokrok, E., Golshan, M.E.H.: 'Adaptive voltage droop scheme for voltage source converters in an islanded multibus microgrid', *IET Gener., Transm. Distrib.*, 2010, **4**, (5), pp. 652–578
4 Bidram, A., Hamedani-golshan, M.E., Davoudi, A.: 'Loading constraints for first swing stability margin enhancement of distributed generation', *IET Gener., Transm. Distrib.*, 2012, **6**, (12), pp. 1292–1300
5 Bidram, A., Hamedani-golshan, M.E., Davoudi, A.: 'Capacitor design considering first swing stability of distributed generations', *IEEE Trans. Power Syst.*, 2012, **27**, (4), pp. 1941–1948
6 Lasseter, R.H.: 'Microgrids'. IEEE Power Engineering Society Winter Meeting, New York, 2002, pp. 305–308
7 Guerrero, J.M., Vásquez, J.C., Matas, J., Castilla, M., Vicuña, L.G.d., Castilla, M.: 'Hierarchical control of droop-controlled AC and DC microgrids – A general approach toward standardization', *IEEE Trans. Ind. Electron.*, 2011, **58**, (1), pp. 158–172
8 Bidram, A., Davoudi, A.: 'Hierarchical structure of microgrids control system', *IEEE Trans. Smart Grid*, 2012, **3**, (4), pp. 1963–1976
9 Sao, C.K., Lehn, W.: 'Control and power management of converter fed microgrids', *IEEE Trans. Power Syst.*, 2008, **23**, (3), pp. 1088–1098
10 Ilic, M.D., Liu, S.X.: 'Hierarchical power systems control: its value in a changing industry' (Springer, London, UK, 1996)
11 Mehrizi-Sani, A., Iravani, R.: 'Potential-function based control of a microgrid in islanded and grid-connected models', *IEEE Trans. Power Syst.*, 2010, **25**, (4), pp. 1883–1891
12 Katiraei, F., Iravani, M.R., Lehn, P.W.: 'Micro-grid autonomous operation during and subsequent to islanding process', *IEEE Trans. Power Deliv.*, 2005, **20**, (1), pp. 248–257
13 Savaghebi, M., Jalilian, A., Vasquez, J., Guerrero, J.: 'Secondary control scheme for voltage unbalance compensation in an islanded droop-controlled microgrid', *IEEE Trans. Smart Grid*, 2010, **3**, (2), pp. 797–807
14 Zhang, Z., Chow, M.: 'Convergence analysis of the incremental cost consensus algorithm under different communication network topologies in a smart grid', *IEEE Trans. Power Syst.*, 2012, **27**, (4), pp. 1761–1768
15 D' Andrea, R., Dullerud, G.E.: 'Distributed control design for spatially interconnected systems', *IEEE Trans. Autom. Control*, 2003, **48**, (9), pp. 1478–1495
16 Xin, H., Qu, Z., Seuss, J., Maknouninejad, A.: 'A self-organizing strategy for power flow control of photovoltaic generators in a distribution network', *IEEE Trans. Power Syst.*, 2011, **26**, (3), pp. 1462–1473
17 Hui, Q., Haddad, W.: 'Distributed nonlinear control algorithms for network consensus', *Automatica*, 2008, **42**, pp. 2375–2381
18 Fax, J., Murray, R.: 'Information flow and cooperative control of vehicle formations', *IEEE Trans. Autom. Control*, 2004, **49**, (9), pp. 1465–1476
19 Ren, W., Beard, R.W.: 'Distributed consensus in multi-vehicle cooperative control' (Springer, Berlin, 2008)
20 Olfati-Saber, R., Murray, R.M.: 'Consensus problems in networks of agents with switching topology and time-delays', *IEEE Trans. Autom. Control*, 2004, **49**, (9), pp. 1520–1533
21 Jadbabaie, A., Lin, J., Morse, A.S.: 'Coordination of groups of mobile autonomous agents using nearest neighbor rules', *IEEE Trans. Autom. Control*, 2003, **48**, (6), pp. 988–1001
22 Li, X., Wang, X., Chen, G.: 'Pinning a complex dynamical network to its equilibrium', *IEEE Trans. Circuits Syst. I: Regular Papers*, 2004, **51**, (10), pp. 2074–2087
23 Li, Z., Duan, Z., Chen, G., Huang, L.: 'Consensus of multi-agent systems and synchronization of complex networks: a unified viewpoint', *IEEE Trans. Circuits Syst. I*, 2010, **57**, (1), pp. 213–224
24 Cady, S.T., Dominguez-Garcia, A.D.: 'Distributed generation control of small-footprint power systems'. Proc. North American Power Symp., 2012, pp. 1–6
25 Wood, A., Wollenberg, B.: 'Power generation, operation, and control' (Wiley, New York, NY, 1996)
26 Pogaku, N., Prodanovic, M., Green, T.C.: 'Modeling, analysis and testing of autonomous operation of an inverter-based microgrid', *IEEE Trans. Power Electron.*, 2007, **22**, (2), pp. 613–625
27 McArthur, S.D.J., Davidson, E.M., Catterson, V.M., *et al.*: 'Multi-agent systems for power engineering applications-part I: concepts, approaches, and technical challenges', *IEEE Trans. Power Syst.*, 2007, **22**, (4), pp. 1743–1752
28 Qu, Z.: 'Cooperative control of dynamical systems: applications to autonomous vehicles' (Springer-Verlag, New York, 2009)
29 Slotine, J.J.E., Li, W.: 'Applied nonlinear control' (Prentice-Hall, New Jersey, 2009)
30 Zhang, H., Lewis, F.L., Das, A.: 'Optimal design for synchronization of cooperative systems: state feedback, observer, and output feedback', *IEEE Trans. Autom. Control*, 2011, **56**, (8), pp. 1948–1952
31 Serban, I., Marinescu, C.: 'Frequency control issues in microgrids with renewable energy resources'. Proc. Seventh Int. Symp. on Advanced Topics in Electrical Eng., 2011, pp. 1–6
32 Bassi, E., Benzi, F., Lusetti, L., Buja, G.S.: 'Communication protocols for electrical drives'. Proc. 21st Int. Conf. Industrial Electronics (IECON), 1995, pp. 706–711
33 Ahuja, R.K., Magnanti, T.L., Orlin, J.B.: 'Network flows: theory, algorithms, and applications' (Prentice-Hall, Englewood Cliffs, 1993)
34 Burkard, R., Dell'Amico, M., Martello, S.: 'Assignment problems' (SIAM, Philadelphia, 2009)